Published in "Physical Review Letters 100: 205701, 2008"
which should be cited to refer to this work.

Quantum Magnets under Pressure: Controlling Elementary Excitations in $TlCuCl_3$

Ch. Rüegg,[1] B. Normand,[2,3] M. Matsumoto,[4] A. Furrer,[5] D. F. McMorrow,[1] K. W. Krämer,[6] H. -U. Güdel,[6] S. N. Gvasaliya,[5] H. Mutka,[7] and M. Boehm[7]

[1]*London Centre for Nanotechnology, University College London, London WC1E 6BT, United Kingdom*
[2]*Département de Physique, Université de Fribourg, CH-1700 Fribourg, Switzerland*
[3]*Theoretische Physik, ETH-Hönggerberg, CH-8093 Zürich, Switzerland*
[4]*Department of Physics, Faculty of Science, Shizuoka University, Shizuoka 422-8529, Japan*
[5]*Laboratory for Neutron Scattering, ETH Zurich and Paul Scherrer Institute, CH-5232 Villigen PSI, Switzerland*
[6]*Department of Chemistry and Biochemistry, University of Bern, CH-3000 Bern 9, Switzerland*
[7]*Institut Laue Langevin, BP 156, 38042 Grenoble Cedex 9, France*

We follow the evolution of the elementary excitations of the quantum antiferromagnet $TlCuCl_3$ through the pressure-induced quantum critical point, which separates a dimer-based quantum disordered phase from a phase of long-ranged magnetic order. We demonstrate by neutron spectroscopy the continuous emergence in the weakly ordered state of a low-lying but massive excitation corresponding to longitudinal fluctuations of the magnetic moment. This mode is not present in a classical description of ordered magnets, but is a direct consequence of the quantum critical point.

PACS numbers: 64.70.Tg, 75.10.Jm, 75.40.Gb, 78.70.Nx

Although quantum fluctuations of both spin and charge degrees of freedom are the key to the essential physics of many challenging problems in condensed matter systems, the microscopic control of zero-point fluctuations has to date remained largely a theoretical abstraction. However, full control over the interaction parameters can now be effected in cold atomic condensates through the standing-wave amplitudes of the optical lattice. Similarly, in quantum magnets the exchange interactions can be controlled by the application of pressure, altering the effect of spin fluctuations. We follow this approach to investigate the physics of a quantum system whose fluctuations are ''tuned'' in a continuous way.

The most dramatic manifestation of such control is the driving of a quantum phase transition [QPT, Fig. 1(a)] between two different ground states [1]. Structurally dimerized $S = 1/2$ spin systems offer a particularly clean realization both of the magnetic field-induced QPT, which has been studied extensively in a number of materials [2], and of the qualitatively different magnetic QPT driven by hydrostatic pressure [3]. The Hamiltonian

$$\mathcal{H} = \sum_i J(p)\mathbf{S}_{i,l}\cdot\mathbf{S}_{i,r} + \sum_{ij;m,m'=l,r} J_{ij}(p)\mathbf{S}_{i,m}\cdot\mathbf{S}_{j,m'} \quad (1)$$

contains pressure-dependent Heisenberg intradimer interactions $J(p)$ and interdimer bonds $J_{ij}(p)$ between spins (l, r) on dimers i and j. Schematically, stabilization of the quantum disordered (QD) phase is driven by spin-singlet formation on the dimer units, while a weakening of this tendency leaves a renormalized classical (RC) phase, whose conventional properties are partially suppressed by dimer fluctuations [4]. Because of its extremely low critical pressure, $p_c = 1.07$ kbar [5], the pressure-induced QPT in $TlCuCl_3$ [6] offers a unique opportunity to study static and dynamic properties throughout the quantum critical regime. Here we determine by high-resolution inelastic neutron scattering (INS) the spin excitation energies, spectral weights, lifetimes, and polarizations.

The QD ground state is a spin singlet with three triplet excitation branches, which are fully gapped and, for a

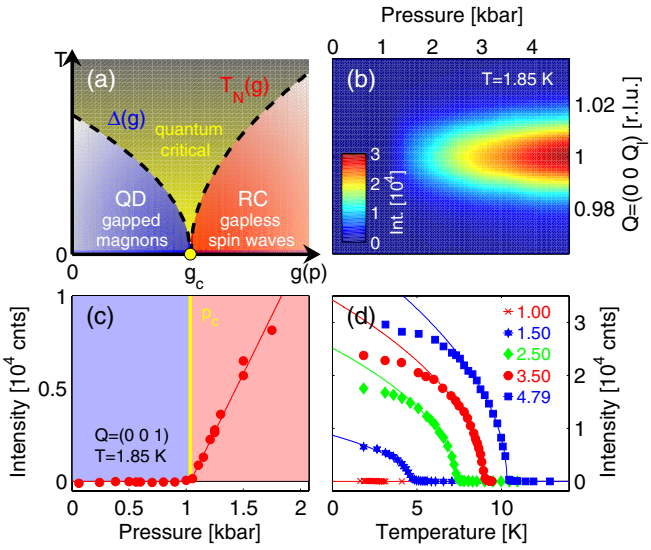

FIG. 1 (color online). (a) Generic phase diagram for a QPT occurring as a function of the parameter $g(p) \propto \sum_j J_{ij}(p)/J(p)$. For a magnetic QPT, the characteristic energy scales in the QD and RC phases are, respectively, the spin gap Δ and Néel temperature T_N, both of which vanish at the QPT. The nature of the lowest-lying excitations is as given. (b)–(d) Pressure and temperature dependence of the magnetic Bragg peak intensity at $\boldsymbol{Q} = (0\ 0\ 1)$ in $TlCuCl_3$, which is proportional to the square of the order parameter m_s.

system with unbroken spin symmetry, degenerate. On the RC side but far from the QPT, one has effectively an ordered state with a rigid magnetic moment, whose key excitations are considered to be only two massless spin waves, the Goldstone modes corresponding to transverse (phase) fluctuations [4,5]. However, the RC phase takes on an increasingly exotic nature close to the continuous QPT, where the hallmarks of ''classical'' behavior are present only as a thin veneer superposed on the dimer-singlet background. We will show that a further low-lying excitation is present in this regime: the missing longitudinal mode [7,8] emerges as the small ordered moment becomes increasingly ''malleable'' on approaching the QPT systematically by controlling the applied pressure. Triplet modes in $TlCuCl_3$ have to date been measured only with rather coarse resolution, in the QD state [9] and deep within the RC phase at 7.3 kbar ($p \gg p_c$) [5], where the spin structure has also been elucidated [10]. Our data now connect these limits, providing unprecedented high-resolution information on the evolution of the excitation spectra across the QPT.

High-quality single crystals of $TlCuCl_3$, with sample mass 1.5 g and a pressure independent mosaic spread of 0.5°, are grown by the Bridgman method. The INS experiments were performed on the triple-axis spectrometers TASP (SINQ) [11] and IN14 (ILL), working in constant final-energy mode with a focusing pyrolytic graphite analyzer and monochromator and respective horizontal collimations 50'-open-open-open and open-60'-open-open. The instruments were operated, respectively, at $E_f =$ 3.5 meV and 3.0 meV, both giving elastic energy resolutions of 0.1 meV FWHM (full width at half maximum height) across the spectral range, and very clean background conditions. A cooled Be filter is positioned between the analyzer and the sample, which was housed in a He-gas pressure cell and in a standard cryostat operating at $T \geq$ 1.5 K. INS measurements detect the components of magnetic fluctuations in the plane perpendicular to the momentum transfer $\boldsymbol{Q}$. Specifically, points $\boldsymbol{Q} = (0\ 0\ 1)$ and $(0\ 4\ 0)$ give access to spin fluctuations in all three spatial directions, and thus for an ordered magnet contain both transverse and longitudinal excitations. The extent to which the individual mode polarizations are present at these wave vectors is determined by the magnetic structure of $TlCuCl_3$ above p_c, and our assignment (below) is fully consistent with the results reported in Ref. [10].

We touch only briefly on static properties. Figures 1(b)–1(d) show the complete pressure and temperature dependences of the ordered moment, m_s, measured through the magnetic Bragg peak intensity. A clear and continuous onset is visible in Fig. 1(b): the QPT is of second order, with a linear pressure dependence [Fig. 1(c)] on the RC side. The temperature dependence shown in Fig. 1(d) is used to extract $T_N(p)$ [5].

Typical INS spectra for the spin excitations in $TlCuCl_3$ are shown in Fig. 2 for a number of pressure values. The

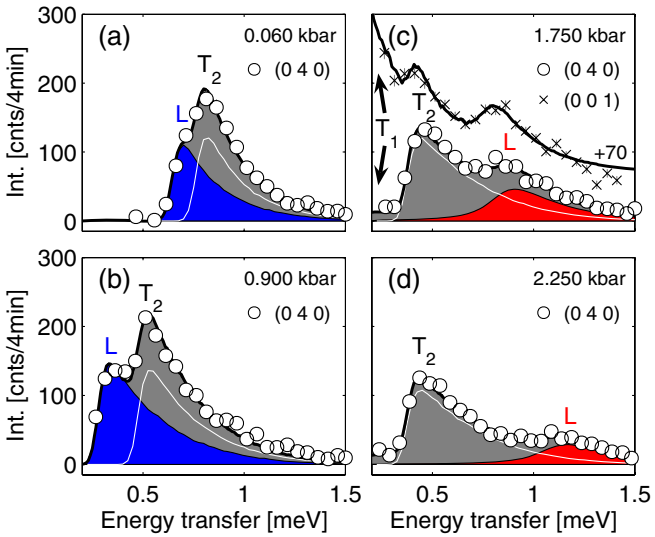

FIG. 2 (color online). INS spectra showing triplet excitations at $T = 1.85$ K and $\boldsymbol{Q} = (0\ 4\ 0)$ for four different pressures across the QPT. Complementary data taken at $\boldsymbol{Q} = (0\ 0\ 1)$ is shown in (c).

INS intensities at the band minimum for $p < p_c$ [Figs. 2(a) and 2(b)] show a closing of the gaps: there are two resolved excitations, labeled T_2 and L. The intensities change dramatically on crossing the QPT [Fig. 2(c)], with T_2 essentially unchanged, an apparently massless mode T_1 becoming visible, and L opening a significant gap. At high pressures [Fig. 2(d)], the low-lying modes (T_1 and T_2) have unchanged energies, whereas the emerging gapped mode L has moved still higher, losing intensity and broadening simultaneously. Figure 3 summarizes the properties of the excitations across the QPT, displaying clearly three key features: (i) there is a low-pressure splitting of the triplet manifold; (ii) the QPT is a second-order transition to within experimental resolution in all quantities measured; (iii) the two transverse spin waves of the ordered phase, one of which is massive, are accompanied by a well-defined longitudinal mode, whose properties change continuously with applied pressure.

Figure 4 presents a complete analysis of the longitudinal mode, beginning with the intensity data [Fig. 4(a)] obtained from the red peaks shown in Figs. 2(c) and 2(d), from which the mode energy [Fig. 4(b)], integrated intensity [Fig. 4(c)], and FWHM [Fig. 4(d)] are extracted. On moving away from the QPT, the mode mass rises monotonically [Fig. 4(b)] and its intensity weakens [Fig. 4(c)], reflecting a larger, stiffer magnetic moment [Fig. 1(c)], and hence a reduced effect of quantum fluctuations. The broadening is always small compared to the mass, and vanishes systematically on approaching the QPT [Fig. 4(d)], suggesting that the longitudinal mode may be an elementary excitation of the ordered system in this regime.

The fits of excitation energies and intensities in Figs. 3 and 4 are obtained from a theoretical model based on the bond-operator technique [4]. A specific representation for the weakly ordered phase is provided by the superposition

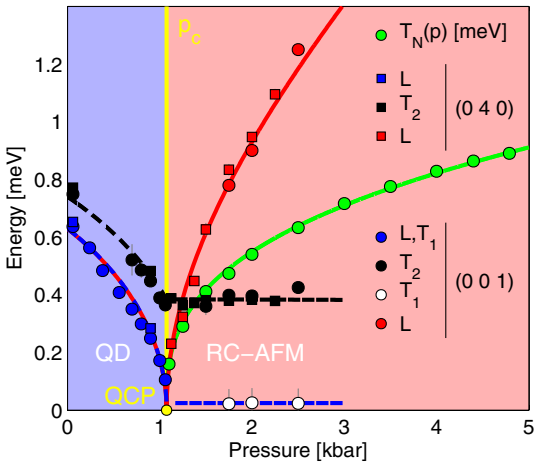

FIG. 3 (color online). Summary of INS results for the gaps of all three triplet excitations as functions of pressure at $T = 1.85$ K. Data for $T_N(p)$ from Ref. [5]. Modes L and T_1 are degenerate within experimental resolution at $p < p_c$. Red symbols show the longitudinal mode L at $p > p_c$. Solid and dashed lines are theoretical fits.

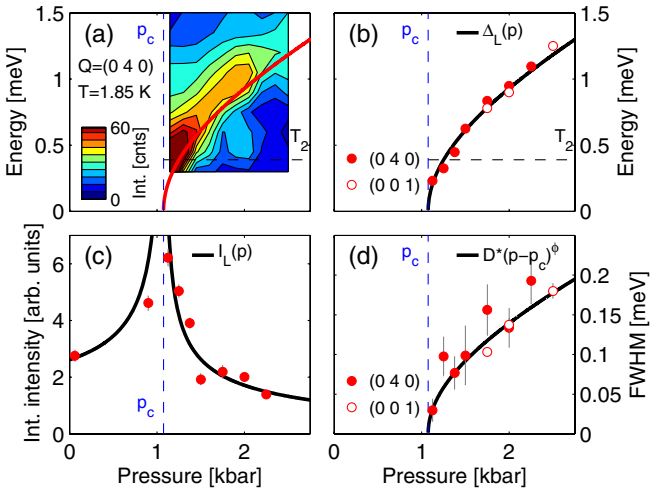

FIG. 4 (color online). Longitudinal mode in the pressure-controlled RC phase. (a) INS intensity as a function of energy for predominantly longitudinal fluctuations (red peaks, Fig. 2) measured at $\boldsymbol{Q} = (0\ 4\ 0)$. (b) Longitudinal mode gap $\Delta_L(p)$: the black curve obtained from the theoretical description has a square-root form, $\Delta_L(p) \propto (p - p_c)^{1/2}$. (c) Integrated scattering intensity, which is inversely proportional to the gap for $p > p_c$. (d) FWHM: here the black line is a guide to the eye, with fitted exponent $\phi = 0.5 \pm 0.1$.

of singlet and triplet states on each dimer bond: the QD state is described by the singlet component ($|s\rangle$), and the properties of the RC phase by an additional triplet component. For the pressure-induced QPT, the wave function $|\sigma_i\rangle$ of a dimer may be written as

$$|\sigma_i\rangle = [\cos\theta|s\rangle + \sin\theta e^{i\boldsymbol{Q}_{AF}\cdot\boldsymbol{r}_i}|t_z\rangle], \qquad (2)$$

where θ increases monotonically with pressure from 0 at $p = p_c$ to $\pi/4$ for perfect antiferromagnetism, $\boldsymbol{Q}_{AF}$ is the ordering wave vector, and $\boldsymbol{r}_i$ the position of dimer i. The triplet mixing coefficient $\sin\theta$ is the sole parameter determining all the physical properties of the ordered state ($T_N(p)$, $m_s(p) = g\mu_B \sin\theta/\sqrt{2}$, $\Delta_L(p)$), and is specified entirely by the pressure evolution of the superexchange parameters. The emergence of the longitudinal mode is contained naturally in this theoretical framework.

The problem of modeling hydrostatic pressure effects in $TlCuCl_3$ is underconstrained. We have fitted the data by assuming both an increase of J_2 (an interdimer coupling in the a-c plane [4]) and a reduction of J. Either change in isolation acts to close the gap and to alter the dispersion, making this linear at the band minimum at the QPT, where a perfectly SU(2)-symmetric system would have three spin waves. The evolution of the mode gaps at $p < p_c$, and the ordered moment and longitudinal mode gap at $p > p_c$, are reproduced with the functional forms $J(p) = J(1 + A_0 p + B_0 p^2)$, $J_2(p) = J_2(1 + A_2 p + B_2 p^2)$. The exponents of the transition are dictated by the linear terms, which were taken as $A_2 = -A_0 = 0.006\,60$ kbar^{-1}, while the quadratic coefficients $B_2 = -B_0 = 0.001\,09$ kbar^{-2} were also necessary to ensure an adequate fit.

Similarly, the anisotropic interactions required to account for the experimental observations may reside on the dimer bonds, on the interdimer bonds, or on both. In a minimal model where only J is anisotropic, one may define uni- and biaxial anisotropy parameters J_{xx} and J_{yz} by $J_x = J + J_{xx}$, $J_{y,z} = J \pm J_{yz}$. The conclusions obtained using interdimer exchange anisotropy are qualitatively identical. The excitation gaps are very sensitive to this anisotropy, which can thus be deduced with extremely high precision from the INS data. The low-pressure data show two resolved mode energies, the best fit giving gaps $\Delta = 0.65$ meV and 0.79 meV. The separation of the upper mode (T_2) is reproduced by an easy-plane, uniaxial anisotropy $J_{xx} = 0.008J$ for pure intradimer anisotropy ($J'_{xx} = -0.004J'$ for pure interdimer anisotropy). At $p > p_c$ we observe (a) one massive "spin-wave" (transverse, T_2) mode with gap $\Delta = 0.38$ meV, (b) one nearly massless transverse mode (T_1) with fitted gap 0.023 meV, and (c) one excitation which becomes higher-lying away from p_c (L). (a) The gap of T_2 is in good agreement with the value 0.8% (-0.4%) for the uniaxial anisotropy component deduced at $p < p_c$. (b) The data correspond to a biaxial anisotropy of 0.002% (-0.001%), a value impossible to resolve at $p < p_c$, and are more appropriately considered as setting an effective upper limit on the possible mass of T_1. (c) The longitudinal mode shows a characteristic pressure evolution where the gap scales with the ordered moment and Néel temperature, following precisely the parameter-free curve in Fig. 4(b). The data for all pressures are described by the same anisotropy, and its value is consistent with that deduced from electron spin resonance measurements [12].

The field-induced QPT, because it involves a U(1)-symmetric order parameter and quadratically dispersing bosons, has been described as a Bose-Einstein condensation (BEC) of the single magnon mode which becomes

massless [2]. Even for precisely uniaxial exchange anisotropy, the pressure-induced transition, where the magnon dispersion is linear, cannot qualify as a BEC and has the scaling exponents of a different universality class. However, from the structure of the theoretical description, the ordered phase remains a ''condensate of magnons''. By the way of further contrast, at the pressure-induced QPT the Goldstone modes are explicitly those triplets not mixing with the singlet, while the linear singlet-triplet combination orthogonal to the ground state [Eq. (2)] becomes massive.

Evidence for longitudinal excitations in quantum magnets has been reported in structures including the $S = 1$ chain compound $CsNiCl_3$ [13] and the $S = 1/2$ chain systems $KCuF_3$ [14] and $BaCu_2Si_2O_7$ [15]. However, the nature of the excitation spectra in these quasi-one-dimensional materials, which are dominated by a spinon-like continuum, is ambiguous to the extent that the existence of the longitudinal mode has been called into question [15] on the grounds that it may decay into spin waves. Our continuous control of the ordered state allows a fully systematic approach to p_c, and it is clear that the longitudinal mode shows no sign of a divergent decay at the QPT [Fig. 4(d)]. In fact the fitted exponent of the decay as a function of pressure, $\phi = 0.5 \pm 0.1$, matches closely the exponent of the gap. For strict equality, the mode could not be called truly elementary, but would be best described as ''critically well-defined.'' That the mode should have precisely this nature at the QPT in a three-dimensional system was deduced in Ref. [16] from the fact that $3 + 1$ is the upper critical dimension in this case. Further measurements over a range of temperatures are required to verify whether this result is a genuine example of quantum critical dynamics.

Our results have a direct connection to the properties of many other quantum spin systems with strong fluctuation phenomena and partially or entirely suppressed magnetism [3]. Excitation spectra have been measured in cases including the $S = 1$ (''Haldane'') chain and two-leg $S = 1/2$ ladder (both QD), and the $S = 1/2$ square lattice (RC, [17]). The QD state of most interest in quantum magnetism is one where the singlets are no longer localized, the resonating valence-bond (RVB) state. While positional resonance may be the mechanism for suppression of order in some highly isotropic models, low-lying triplet states are a generic feature of any system near a magnetic QPT. Excitation spectra in the RVB framework have been discussed explicitly for the square lattice [18], and the same approach to other models would reveal emergent low-lying modes in RVB states. This type of investigation may be realized not only in spin systems under pressure, for example, in the highly frustrated kagome geometry [19], but also in cold fermionic systems on optical lattices [20]. Finally, several theories for high-temperature superconductivity are based on the existence of a QPT [3,21] occurring as a function of hole doping. Our results deliver the clear message that a complete account of the excitation spectrum is an integral part of establishing the validity of such a scenario.

In summary, we have performed high-resolution neutron spectroscopy on the quantum antiferromagnet $TlCuCl_3$ over a range of applied pressure values across the magnetic quantum phase transition. We demonstrate the continuous evolution of the spin dynamics and drive the emergence of a critically well-defined longitudinal excitation (amplitude mode) of the ordered moment in the renormalized classical phase. A theoretical framework is developed which describes the measured excitations in all regions of the phase diagram. We use this systematic experimental control of the quantum state to illustrate in every detail the profound connection between the excitations of phases separated by a quantum critical point.

We thank T. M. Rice and M. Sigrist for invaluable contributions. We are grateful to G. Aeppli, C. Batista, M. Vojta, and M. Zhitomirsky for helpful comments. This work was performed in part at the Swiss spallation neutron source, SINQ, at the Paul Scherrer Institute, and was supported by the Swiss National Science Foundation, the NCCR MaNEP, and the Wolfson Foundation.

[1] S. Chakravarty, B. I. Halperin, and D. R. Nelson, Phys. Rev. B **39**, 2344 (1989).
[2] T. Giamarchi, Ch. Rüegg, and O. Tchernyshyov, Nature Phys. **4**, 198 (2008).
[3] S. Sachdev, Nature Phys. **4**, 173 (2008).
[4] M. Matsumoto, B. Normand, T. M. Rice, and M. Sigrist, Phys. Rev. B **69**, 054423 (2004).
[5] Ch. Rüegg *et al.*, Phys. Rev. Lett. **93**, 257201 (2004).
[6] H. Tanaka *et al.*, Physica (Amsterdam) **329–333B**, 697 (2003).
[7] I. Affleck, Phys. Rev. Lett. **62**, 474 (1989).
[8] B. Normand and T. M. Rice, Phys. Rev. B **56**, 8760 (1997).
[9] N. Cavadini *et al.*, Phys. Rev. B **63**, 172414 (2001).
[10] A. Oosawa *et al.*, J. Phys. Soc. Jpn. **73**, 1446 (2004).
[11] F. Semadeni, B. Roessli, and P. Böni, Physica (Amsterdam) **297B**, 152 (2001).
[12] A. K. Kolezhuk, V. N. Glazkov, H. Tanaka, and A. Oosawa, Phys. Rev. B **70**, 020403 (2004).
[13] M. Kenzelmann *et al.*, Phys. Rev. B **66**, 024407 (2002).
[14] B. Lake, D. A. Tennant, and S. Nagler, Phys. Rev. B **71**, 134412 (2005).
[15] A. Zheludev, K. Kakurai, T. Masuda, K. Uchinokura, and K. Nakajima, Phys. Rev. Lett. **89**, 197205 (2002).
[16] I. Affleck and G. F. Wellman, Phys. Rev. B **46**, 8934 (1992).
[17] N. B. Christensen *et al.*, Proc. Natl. Acad. Sci. U.S.A. **104**, 15 264 (2007).
[18] C.-M. Ho, V. Muthukmar, M. Ogata, and P. W. Anderson, Phys. Rev. Lett. **86**, 1626 (2001).
[19] J. S. Helton *et al.*, Phys. Rev. Lett. **98**, 107204 (2007).
[20] S. Trebst, U. Schollwöck, M. Troyer, and P. Zoller, Phys. Rev. Lett. **96**, 250402 (2006).
[21] S. Sachdev, Rev. Mod. Phys. **75**, 913 (2003).